2. Magnetic Properties:

In the preceding introductory chapter we focused more on the electrical property of a superconductor that its electrical resistance ϱ vanishes below a critical temperature T_c. In the following we discuss that a superconductor differs from an ideal conductor as its magnetic properties are additionally decisive. Namely, it turns out that a superconductor also represents an ideal diamagnet as it expells magnetic flux lines.

2.1 Meissner-Ochsenfeld Effect:

An ideal conductor is described by the Maxwell equations in matter with a vanishing electrical resistance ϱ. From this we can draw the following two conclusions:

1. Ohm law (matter equation): The current density $\vec{j}$ is proportional to the electric field $\vec{E}$

$$\vec{j} = \sigma \vec{E} \tag{2.1}$$

with the conductivity $\sigma = 1/\varrho$ being the proportionality constant. Thus, in the limit of vanishing resistance ϱ we obtain

$$\lim_{\varrho \to 0} \vec{E} = \lim_{\varrho \to 0} \varrho \vec{j} = \vec{0} \tag{2.2}$$

2. Induction law (Maxwell equation): The rotation density of the electric field $\vec{E}$, i.e. $\mathrm{rot}\,\vec{E}$, is given by the negative (Lenz law) of the time derivative of the magnetic induction $\vec{B}$:

$$\mathrm{rot}\,\vec{E} = -\frac{\partial \vec{B}}{\partial t} \tag{2.3}$$

Inserting (2.2) in (2.3) yields

$$\lim_{\varrho \to 0} \frac{\partial \vec{B}}{\partial t} = \vec{0} \tag{2.4}$$

This means that in the loop of an ideal conductor we do not have any induction voltage as the magnetic flux through does not change.

But, in contrast to (2.4), Meissner and Ochsenfeld discovered experimentally in 1933 that the magnetic

induction $\vec{B}$ vanishes inside a superconductor:

$$\vec{B} = \vec{0} \qquad (2.5)$$

This finding differs from (2.4) and can not be explained within the realm of classical physics.

We now compare the behaviour of an ideal conductor with the one of a superconductor within a gedanken-experiment. To this end we consider a cycle process within the B–T phase diagram as shown on the right. For simplicity we restrict ourselves to a spherical body as it can be shown that the magnetic field inside is homogeneous, see section 2.4 below.

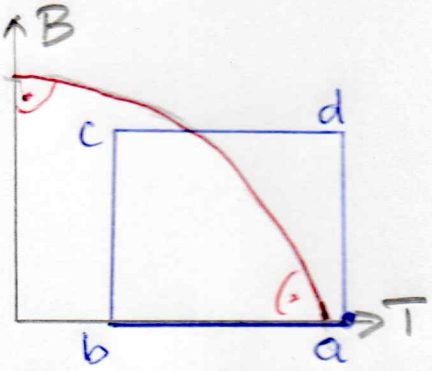

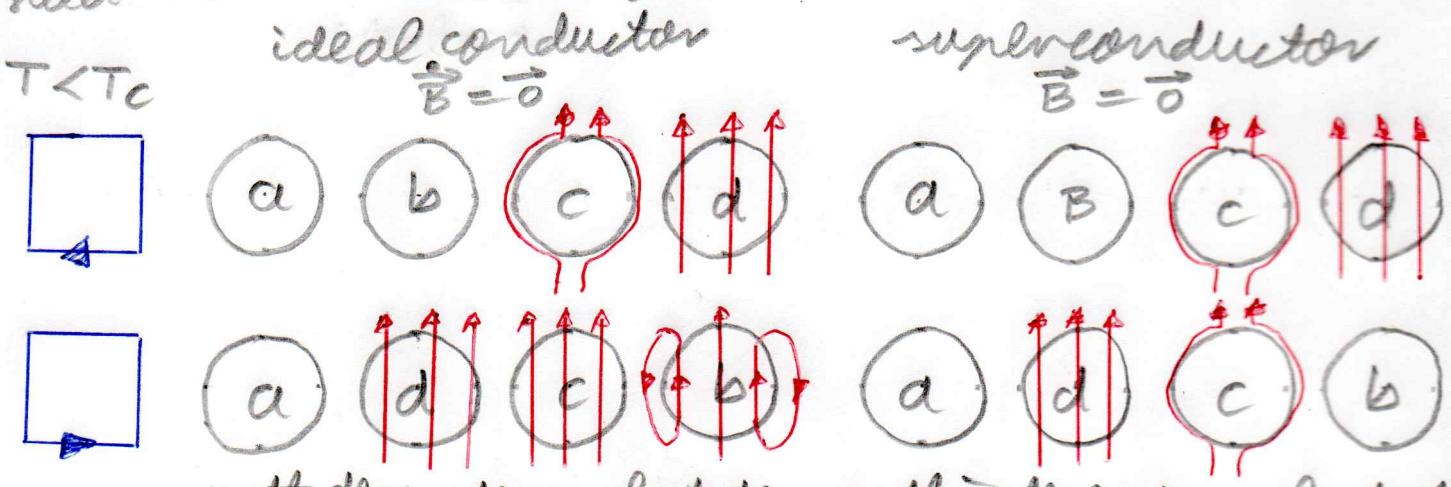

path dependence of state path independence of states

Thus, we can draw the following far-reaching conclusions:

1. The Meissner-Ochsenfeld effect guarantees that a state in a superconductor is path independent. Therefore, it is possible to describe superconductivity within the phenomenological approach of thermodynamics as is discussed in chapter 3.
2. As the behaviour of a superconductor differs from an ideal conductor, the superconducting state can not only be described by the Maxwell equations alone. They must be generalised by the London equations as is worked out in chapter 4.

Let us briefly mention the physical origin of the Meissner-Ochsenfeld effect. It stems from the fact that within a skin of about 100 Å at the surface of a su-

perconductor currents of Cooper pairs persist. Due to the mobility of the Cooper pairs their currents adjust themselves such that the magnetic field vanishes inside the superconductor. In that sense one can call a superconductor an ideal diamagnet.

2.2 Type I Superconductor:

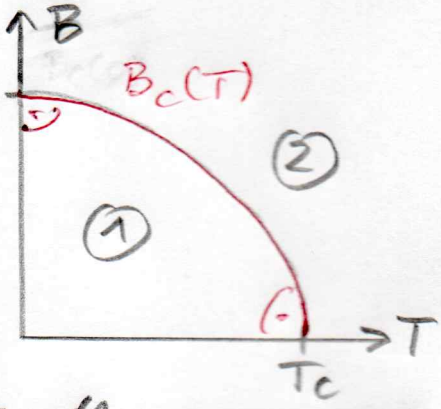

A superconductor of type I has two phases. The superconducting phase ① shows in the volume the Meissner-Ochsenfeld effect. And ② represents the normal conducting phase. Note that the transition line between both phases is described in good approximation by the formula of Gorter (1.3). Furthermore, we remark that we neglect in the following discussion the shape of the body, which usually leads to the so-called stray field. As we will see below in section 2.4 this corresponds approximately to the situation of an infinitely long cylinder.

In matter the magnetic induction $\vec{B}$ consists of two contributions:

$$\vec{B} = \vec{B}_{ext} + \vec{B}_{int} \tag{2.6}$$

The first one comes from the magnetic field $\vec{H}$ impressed from outside

$$\vec{B}_{ext} = \mu_0 \vec{H} \tag{2.7}$$

The second one describes the impact of matter in terms of the magnetization $\vec{M}$, which stems from the alignment of the elementary magnets in the volume. In case that we have an infinitely large volume we have

$$\vec{B}_{int} = \mu_0 \vec{M} \tag{2.8}$$

The Lorentz force of a magnetic field upon a moving electrical charge depends on the magnetic induction $\vec{B}$. Thus, the Lorentz force does not discriminate whether the physical origin of the magnetic field originates from $\vec{H}$ or from $\vec{M}$.

In matter the magnetization $\vec{m}$ is proportional to the external magnetic field $\vec{H}$, which defines the magnetic susceptibility χ_m:

$$\vec{m} = \chi_m \vec{H} \qquad (2.9)$$

Thus, from (2.6)-(2.9) we conclude

$$\vec{B} = \mu_0 (1 + \chi_m) \vec{H} \qquad (2.10)$$

The Meissner-Ochsenfeld effect (2.5) has then the consequence that the magnetic susceptibility of a superconductor is fixed by

$$\vec{B} = \vec{0} \xrightarrow{(2.10)} \chi_m = -1 \qquad (2.11)$$

This is the defining property of an ideal diamagnet.

In contrast to that the magnetic susceptibility in the normal conducting state stems from paramagnetism. Typically this leads to a value of about $\chi_m \approx 10^{-5}$, which is negligibly small in comparison to (2.11). Thus, we have approximately in the normal conducting state

$$\chi_m \approx 0 \qquad (2.12)$$

The results (2.11) and (2.12) can now be summarized by magnetization curves. Here two representations are possible:

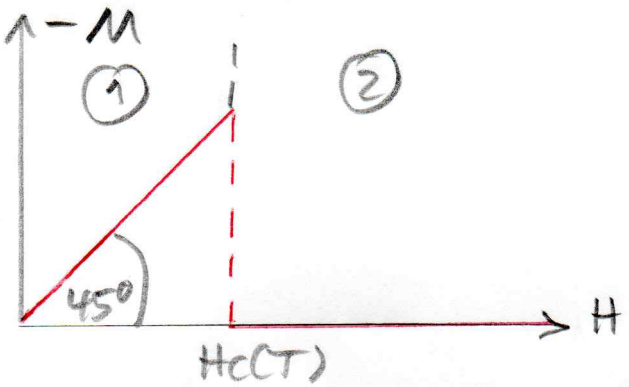

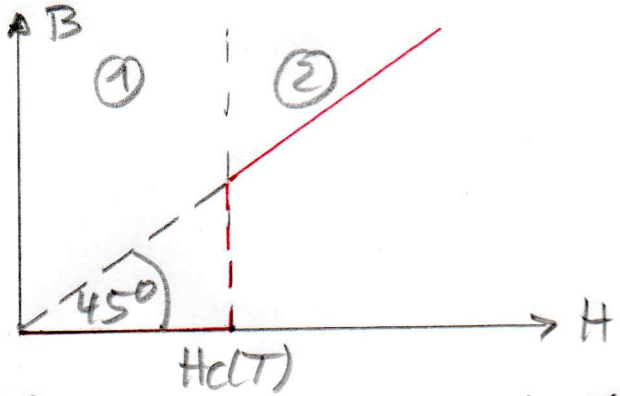

Below we list some examples of type I superconductors together with their respective critical magnetic fields at zero temperature:

element	abbreviation	atomic number	$B_c(0) = \mu_0 H_c(0)$ in T
lead	Pb	82	0.0803
tantalium	Ta	73	0.0830
aluminium	Al	13	0.0990
vanadium	V	23	0.131

Thus, we conclude that the critical magnetic fields of type I superconductors are small.

2.3 Type II Superconductors:

A superconductor of type II has in total 4 phases in the B-T plane of control parameters. The Meissner phase ① shows in the volume the Meissner-Ochsenfeld effect. There the magnetic flux is completely expelled from the superconductor. The Shubnikov phase ② represents a mixed state, where a hexagonal lattice of flux lines exist:

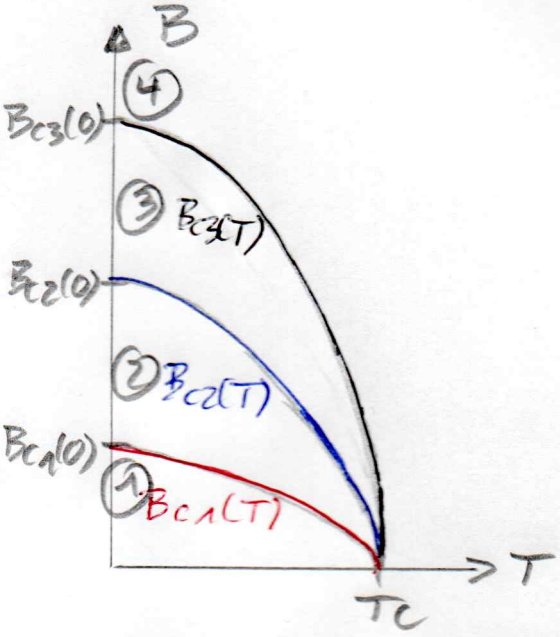

This line illustrates electrodynamically induced interaction forces between two flux quanta.

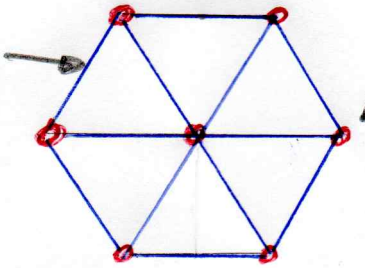

Inside a flux quant a completely normal conducting region exists.

In the surface phase ③ superconductivity only exists at the surface. And ④ represents the normal conducting phase.

Note that the 4 phases are separated by 3 transition lines. Here $B_{c1}(T)$, $B_{c2}(T)$, $B_{c3}(T)$ are called lower and upper critical magnetic field as well as critical magnetic field of surface superconductivity. All three of them follow the Tc approximation (1.3) with the same critical temperature T_c:

$$\frac{B_i(T)}{B_{ci}(0)} = 1 - \left(\frac{T}{T_c}\right)^2 \quad ; \quad i = 1, 2, 3 \qquad (2.13)$$

Let us now describe in more detail the respective magnetic properties of all 4 phases:

① Meissner phase [$0 \leq B \leq B_{c1}(T)$]:
Here we have ideal diamagnetism, which is characterised by (2.11).

② Shubnikov phase [$B_{c1}(T) \leq B \leq B_{c2}(T)$]:
With increasing the external magnetic field strength the number of flux lines also increases. As the inner region of each flux line is normal conducting, i.e. we have there $\chi_m = 0$, the total normal region increases. Thus is the consequence that the magnetization M decreases with increasing the external magnetic field.

③ Surface phase [$B_{c2}(T) \leq B \leq B_{c3}(T)$]:
As the whole volume is already superconducting, the magnetization is already zero, i.e. $M = 0$.

④ Normal conducting phase [$B_{c3}(T) \leq B$]:
Here we have paramagnetism, which yields for all practical purposes $\chi_m = 0$.

Also for type II superconductors there are two possible representations for magnetization curves:

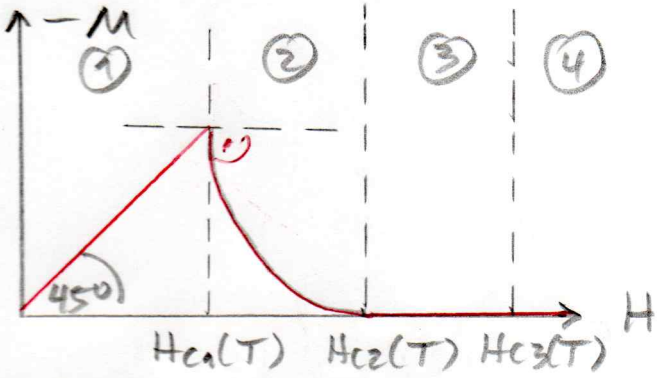

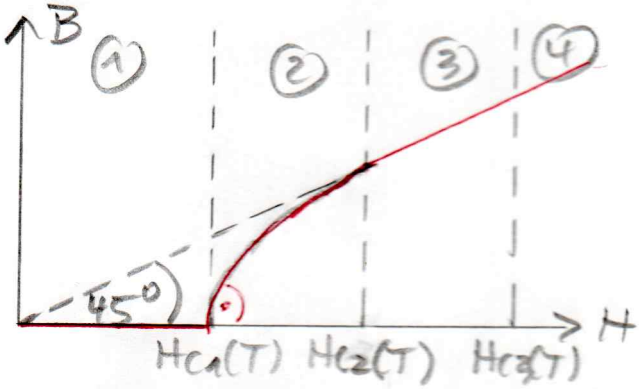

Some examples of type II superconductors together with their upper critical magnetic fields at zero temperature are listed below:

material	Nb	NbTi	Nb_3Sn	$YBa_2Cu_3O_7$
$B_{c2}(0) = \mu_0 H_{c2}(T)$ in T	0.1944	14	25	$\sim 10^2$

Thus, we conclude that the critical magnetic fields of type II superconductors are larger than the critical magnetic fields of type I superconductors. Therefore, type I (II) superconductors are called soft (hard) superconductors.

2.4 Description of Complete Diamagnetism

Here we investigate how the shape of the probe affects the magnetization curves of type I superconductors.

2.4.1 Physical Picture:

To this end we start with describing the underlying physical picture by the example of a homogeneous sphere of a superconducting material:

1. The sphere is put into an external magnetic field $\vec{B}_{ext} = \mu_0 \vec{H}$.
2. At the surface of the sphere surface currents of superconducting (Cooper pairs emerge. This leads to a magnetization $\vec{M}$, which is pointing opposite to the external magnetic field $\vec{H}$ due to the diamagnetic properties of the superconductor.
3. Due to the magnetization $\vec{M}$ effective magnetic charges emerge at the surface of the sphere. As the magnetization $\vec{M}$ is pointing from the south pole to the north pole, a stray field H_S emerges as indicated in the figure, which points inside the sphere parallel to the external magnetic field.
4. Superimposing all three field contributions yields a magnetic induction $\vec{B}$ as indicated in the figure.

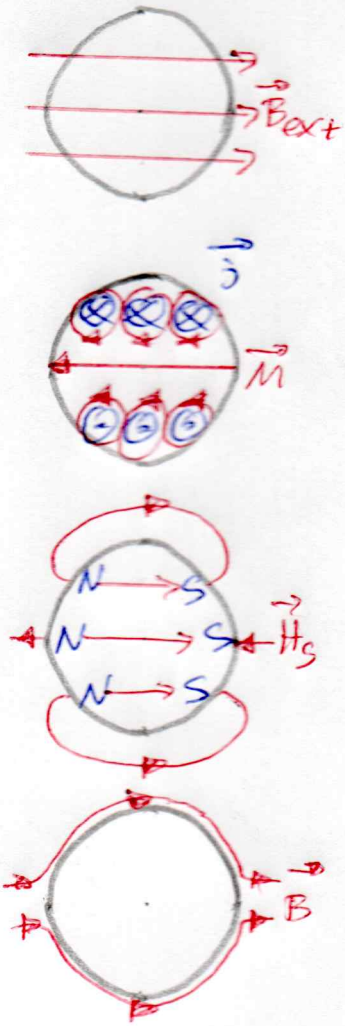

2.4.2 Stray Field:

Now we describe this situation quantitatively. Again the magnetic induction $\vec{B}$ decomposes according to (2.6) with the external magnetic field (2.7). But now we have to generalize (2.8), which is only valid for an infinitely large volume, to a finite probe:

$$\vec{B}_{int} = \mu_0 (\vec{M} + \vec{H}_S) \qquad (2.14)$$

Here the stray field $\vec{H}_S$, which is also called demagnetization field, is discussed in more detail, for instance in the book Amikam Aharoni, Introduction to the Theory of Ferromagnetism, see there chapter 6. For homogeneous magnetization $\vec{M}$ inside the probe the resulting stray field $\vec{H}_S$ is given by

$$\vec{H}_S = -N\,\vec{M} \qquad (2.15)$$

Thus, the minus sign guarantees that $\vec{H}_S$, which originates from a surface effect, points opposite to the magnetization $\vec{M}$, which stems from a volume effect. Furthermore, N denotes the demagnetization tensor, which reads

$$N_{ij} = \frac{-1}{4\pi} \int_{\partial V} dF_j' \frac{\partial}{\partial x_i'} \frac{1}{|\vec{r} - \vec{r}'|} \qquad (2.16)$$

with the integral encompassing the whole surface ∂V of the volume V of the probe. Note the useful property that the trace over the demagnetization tensor is always unity:

$$\mathrm{Tr}\, N = N_{ii} = \frac{-1}{4\pi} \int_{\partial V} dF_i' \frac{\partial}{\partial x_i'} \frac{1}{|\vec{r} - \vec{r}'|} = \frac{-1}{4\pi} \int_{\partial V} d\vec{F}' \,\mathrm{grad}' \frac{1}{|\vec{r} - \vec{r}'|}$$

$$\overset{\text{Gauss law}}{=} \frac{-1}{4\pi} \int_V dV' \,\Delta' \frac{1}{|\vec{r} - \vec{r}'|} \overset{\text{Coulomb potential = Green function}}{=} \int_V dV' \,\delta(\vec{r} - \vec{r}') = 1 \qquad (2.17)$$

Here we have used the fact that the coordinate $\vec{r}$ is inside the volume V'.

In principle, the demagnetization tensor N_{ij} can be directly calculated for each probe by evaluating the integral (2.16). However, the trace property (2.17) together with symmetry arguments can be used to determine much easier the demagnetization tensor for the following probe shapes:

1. Infinitely thin layer:
   - $N_2 = N_3 = 0$: magnetic surface charges vanish at infinity.
   - $N_1 + N_2 + N_3 = 0 \Rightarrow N_1 = 1$

$$N = \begin{pmatrix} 1 & 0 & 0 \\ 0 & 0 & 0 \\ 0 & 0 & 0 \end{pmatrix} \qquad (2.18)$$

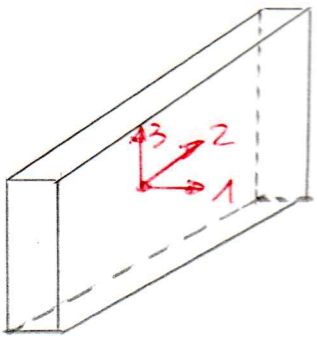

2. Infinitely long cylinder:
   - $N_1 = 0$, see point 1
   - $N_2 = N_3$ due to symmetry
   - $N_1 + N_2 + N_3 = 1 \Rightarrow N_2 = N_3 = 1/2$

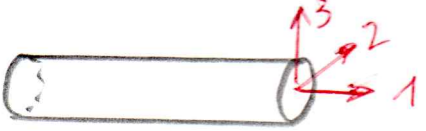

$$N = \begin{pmatrix} 0 & 0 & 0 \\ 0 & 1/2 & 0 \\ 0 & 0 & 1/2 \end{pmatrix} \qquad (2.19)$$

3. Sphere:

- $N_1 = N_2 = N_3$ due to symmetry
- $N_1 + N_2 + N_3 = 1 \Rightarrow N_1 = N_2 = N_3 = \frac{1}{3}$

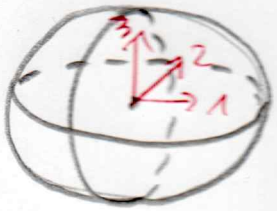

$$N = \begin{pmatrix} 1/3 & 0 & 0 \\ 0 & 1/3 & 0 \\ 0 & 0 & 1/3 \end{pmatrix} \tag{2.20}$$

With this we are equipped to study how the probe shape affects the Meissner-Ochsenfeld effect. To this end we insert (2.7), (2.14), and (2.15) into (2.6) for a particular direction of the external magnetic field:

$$B = \mu_0 (H + M - N M) \tag{2.21}$$

As the magnetic induction has to vanish inside the probe due to the Meissner-Ochsenfeld effect (2.5), we conclude:

$$B = 0 \quad \overset{(2.21)}{\Rightarrow} \quad M(H) = -\frac{1}{1-N} H \tag{2.22}$$

The slope of the magnetization M with respect to the magnetic field H defines the magnetic susceptibility

$$\chi \overset{(2.9)}{=} \frac{\partial M(H)}{\partial H} \overset{(2.22)}{=} -\frac{1}{1-N} \tag{2.23}$$

Thus, we read off from (2.23) that the probe shape and, therefore, the demagnetization N yield an increase of the absolute value of the magnetic susceptibility. As the demagnetization N is limited due to the trace property (2.17) via $0 \leq N \leq 1$, the magnetic susceptibility χ turns out to have the range of values $-\infty < \chi \leq -1$.

Another point of view is provided by the following consideration. From (2.21) we read off that both the external magnetic field H and the stray field $H_S = -NM$ yield an effective inner magnetic induction B_{eff}:

$$B_{eff} = \mu_0 (H + H_S) \overset{(2.15)}{=} \mu_0 (H - NM) \tag{2.24}$$

Inserting therein (2.22), we obtain

$$B_{eff}(H) = \mu_0 \frac{1}{1-N} H \tag{2.25}$$

In case of $N = 0$ the effective inner magnetic induction $B_{eff}(H)$ coincides with the external magnetic induction $\mu_0 H$. But in case of $0 < N \leq 1$ the effective inner magnetic induction $B_{eff}(H)$ is larger than the external magnetic induction $\mu_0 H$. For instance, for a sphere with $N = 1/3$ we obtain from (2.25)

$$B_{eff}^{sphere}(H) = \mu_0 \frac{3}{2} H \qquad (2.26)$$

Furthermore, we observe that the effective inner magnetic induction (2.25) and the magnetization M from (2.22) are related via

$$B_{eff} = -\mu_0 M \qquad (2.27)$$

Thus, we conclude on formal grounds in analogy to (2.9):

$$\chi_{eff} = \mu_0 \frac{\partial M}{\partial B_{eff}} = -1 \qquad (2.28)$$

Thus, the introduction of the effective magnetic induction B_{eff} allows to describe also a finite probe via an effective complete diamagnetism.

2.4.3 Intermediate State:

A consistency problem emerges when the effective magnetic induction B_{eff} in (2.25) inside the probe reaches the external critical field $B_c = \mu_0 H_c$:

$$\mu_0 H_c = \mu_0 \frac{1}{1-N} H_c \quad \Rightarrow \quad 1 = \frac{1}{1-N} \qquad (2.29)$$

Obviously (2.29) can not be fulfilled for $0 < N \leq 1$. Thus, on the one hand, a homogeneous superconducting state is no longer possible. But on the other hand, a homogeneous normal conducting state is also not possible as this would imply $\chi_m = M = 0$ in contradiction to (2.23). This dilemma was solved by Peierls and London in 1936 by concluding that neither a homogeneous superconducting nor a homogeneous normal conducting state exists at $B_{eff} = B_c$. Instead, at $B_{eff} \geq B_c$ the probe realizes an inhomogeneous intermediate state, where the probe is divided into normal and superconducting regions as follows:

1. At $B_{eff} = B_c$ the normal conducting regions occur at first at the equator and then continue from there into the inner of the probe. The reason for this is that the s–n border area, and thus the energy to create it, is minimal at the equator.

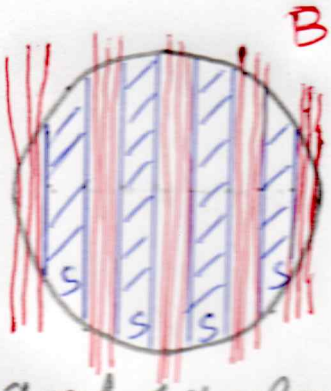

2. The phase boundaries between normal and superconducting regions are always parallel to the magnetic field.
3. The whole structure of the intermediate state follows from minimizing the total energy. This has two consequences:
   a. At $B_{eff} \gtrsim B_c$ only few s–n border areas exist, thus the coexisting normal and superconducting regions are large. Whereas a type II superconductor has only one flux quantum for one flux line, the normal conducting regions of the intermediate state of a type I superconductor involve hundred thousands of flux quanta.
   b. To be more precise, the intermediate state does not exactly emerge at $B_{eff} = B_c$ but at a slightly larger magnetic field as a certain magnetic field energy is necessary to create the s–n border area. But in the following we neglect this additional effect for simplicity.

The normal and the superconducting regions of the intermediate state are characterised by different magnetic properties:

normal conducting region	$B_n = \mu_0 H \geq B_c$	$M_n = 0$
superconducting region	$B_s = 0$	$M_s \overset{(2.22)}{=\!=} -\frac{1}{1-N} H$

Thus, for an inhomogeneous intermediate state one can only talk about spatially averaged magnetic quantities. This allows us now to define an averaged magnetization as the probe response as follows.

The homogeneous superconducting state is characterized due to Meissner-Ochsenfeld effect by the magnetization (2.22) and the effective magnetic induction $B_{eff}(H)$ in (2.25). The transition point to the intermediate state is now given by that magnetic field $H_{cI} \leq H_c$, which fulfills

$$B_{eff}(H_{cI}) = \mu_0 H_c \tag{2.30}$$

Thus, inserting (2.25) into (2.30) yields the critical magnetic field

$$H_{cI} = (1-N) H_c \tag{2.31}$$

It is, indeed, smaller than or equal to H_c due to the range of values of the demagnetization: $0 < N \leq 1$. Furthermore, we conclude that the critical magnetization at the onset of the intermediate state is given by

$$M_{cI} \overset{(2.22)}{=\!=} -\frac{1}{1-N} H_{cI} \overset{(2.31)}{=\!=} -H_c \tag{2.32}$$

We now describe the magnetic properties of the inhomogeneous intermediate state. As we have there both normal and superconducting regions, the effective magnetic induction (2.24) has to be generalized to

$$\tilde{B}_{eff}(H) = \mu_0 (H - N \tilde{M}) \tag{2.33}$$

Here the tilde denotes explicitly the spatial averaging procedure. And the intermediate state is now characterized by the condition that this spatially averaged magnetic induction (2.33) is determined by the critical magnetic field

$$\tilde{B}_{eff}(H) = \mu_0 H_c \tag{2.34}$$

Thus, combining (2.33) and (2.34) yields for the averaged magnetization

$$\tilde{M}(H) = \frac{H - H_c}{N} \tag{2.35}$$

On the one hand, we regain with this the magnetization at the onset of the intermediate state

$$\tilde{M}(H_{cI}) \overset{(2.31),(2.35)}{=\!=} -H_c \;\hat{=}\; (2.32) \;\checkmark \tag{2.36}$$

On the other hand, we find that the averaged magnetization $\tilde{M}(H)$ vanishes at $H = H_c$:

$$\tilde{M}(H_c) \overset{(2.35)}{=} 0 \qquad (2.37)$$

which describes the transition of the intermediate state to the normal conducting state. Thus, the resulting magnetization curve looks as follows

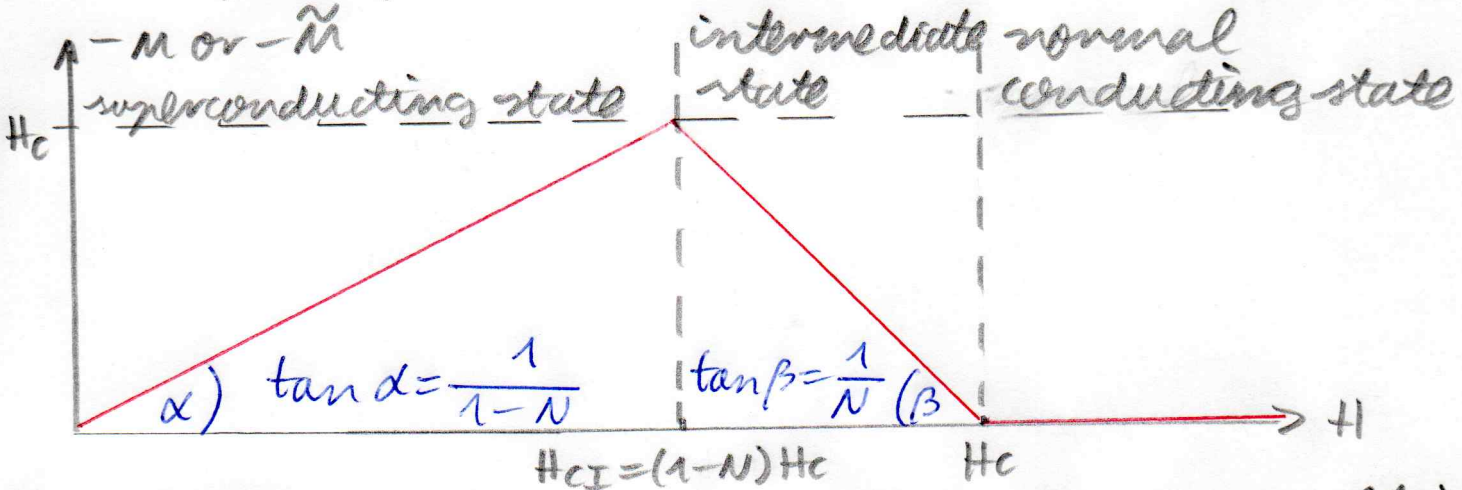

For different demagnetization factors N one obtains different magnetization curves:

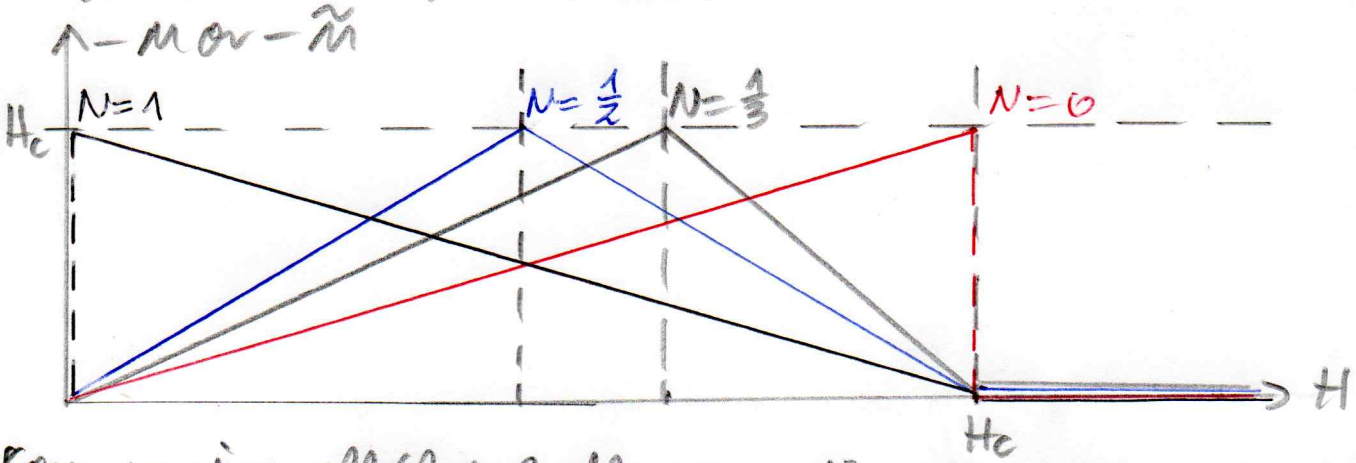

Comparing all these demagnetization curves, we recognize that the areas below the triangles are equal. As all triangles have the same base line H_c and the same height H_c, their resulting area amounts to $H_c^2/2$. This area corresponds to the energy difference between the superconducting and the normal conducting phase. It turns out to be independent of the demagnetization factor N and, thus, independent of the probe shape:

$$E_n - E_s = -\mu_0 \int M(H)\, dH = \frac{\mu_0}{2} H_c^2 = \frac{B_c^2}{2\mu_0} V \qquad (2.38)$$

Thus, the superconducting state has a lower magnetic energy, which is called condensation energy. In

the microscopic picture of the BCS theory, this energy gain results from the condensation of single electrons at the surface of the Fermisphere to Cooper pairs.

Now we determine the magnetic induction B. Due to the Meissner-Ochsenfeld effect (2.5) it vanishes in the superconducting state. In the inhomogeneous intermediate state the spatially averaged magnetic induction reads in analogy to (2.21):

$$\tilde{B} = \mu_0 [H + (1-N)\tilde{M}] \tag{2.39}$$

Inserting (2.35) into (2.39) then yields

$$\tilde{B}(H) = \mu_0 \left[\frac{1}{N} H + \left(1 - \frac{1}{N}\right) H_c\right] \tag{2.40}$$

Thus, at the onset of the intermediate state we obtain an agreement with the Meissner-Ochsenfeld effect:

$$\tilde{B}(H_{cI}) \overset{(2.31),(2.40)}{=\!=} 0 \tag{2.41}$$

Furthermore, we find at H_c

$$\tilde{B}(H_c) \overset{(2.40)}{=\!=} \mu_0 H_c \tag{2.42}$$

so that the magnetic induction goes over continuously into that of the normal conducting state

$$B(H) = \mu_0 H \tag{2.43}$$

Thus, we can summarise these findings in the demagnetization curve

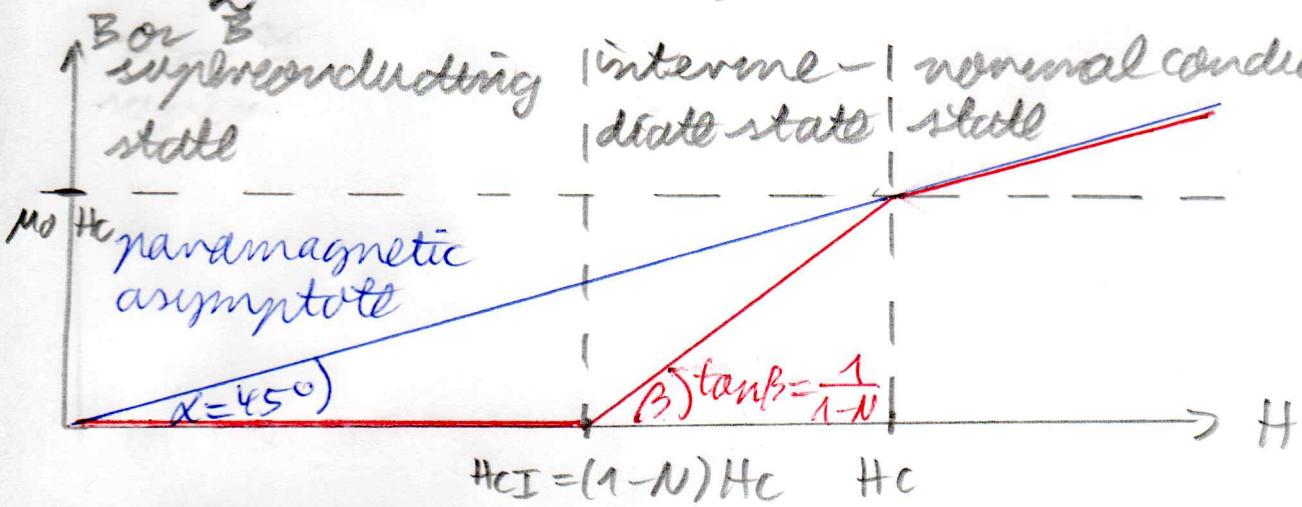

For different demagnetization factors N these magnetization curve have the following form

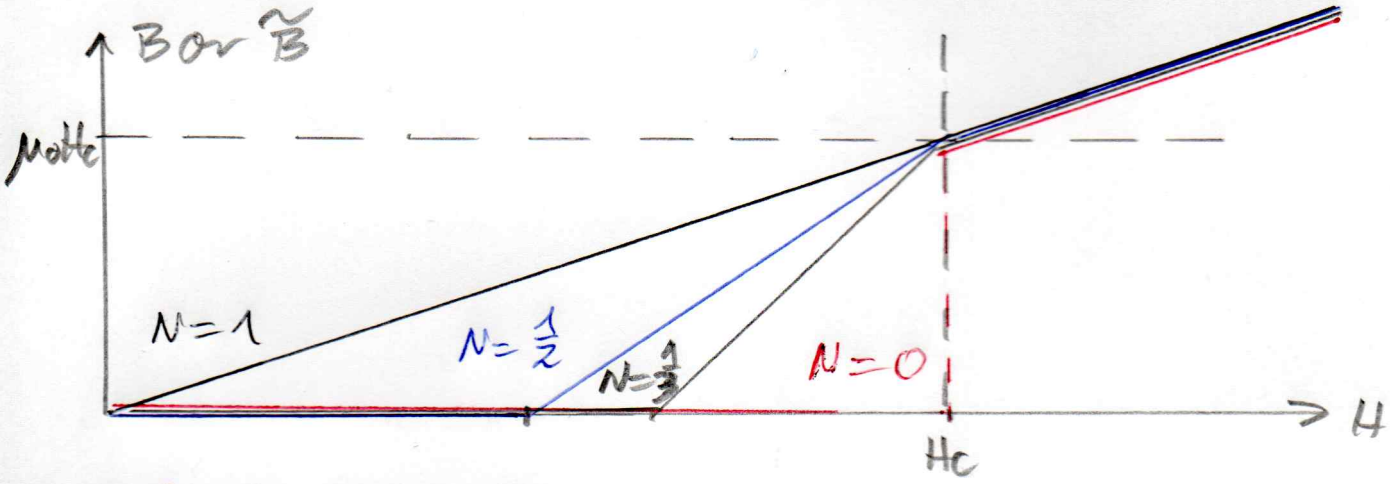

2.5 Experiments:

Here we briefly review three breakthrough experiments, which allowed to investigate the peculiar magnetic properties of superconductors.

2.5.1 Iron Colloids:

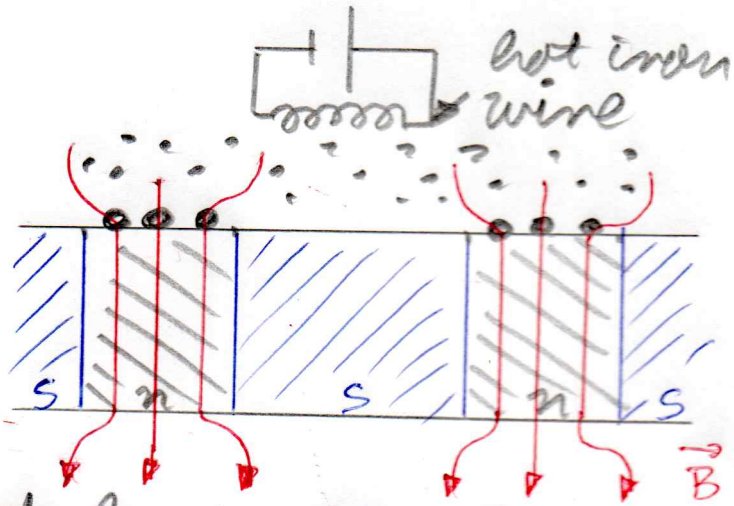

Above a superconducting probe iron is vaporized from a hot wire. The iron atoms diffuse through the helium gas of the cryostat, which stabilizes the temperature in the Kelvin regime and build iron colloids. Those colloids have a diameter of smaller than 50 nm and sediment in helium slowly at the surface of the superconductor. The ferromagnetic iron colloids accumulate at the normal conducting regions as there the magnetic field is largest. And finally, the iron colloids are visualized with an electron microscope.

With this experimental procedure Essmann and Träuble could detect at the Max-Planck Institute of Solid State Physics in Stuttgart in 1966 the intermediate state in superconductors of type I and in 1968 the flux lattice of the mixed state in superconductors of type II.

2.5.2 Niobium Powder:

Another method is based on investigating a super-

conducting probe in the intermediate state with a fine powder of a superconducting material. Which requirements follow for both the probe and the powder? Most importantly, the powder must be superconducting when the type I superconductor is in the intermediate state. This requires the magnetic field of the powder to be larger than the critical magnetic field of the probe:

$$B_c(\text{probe}) < B_c(\text{powder}) \qquad (2.44)$$

Due to the 1st approximation of the transition line (1.3) in the B–T phase diagram this implies that the critical temperature of the powder must be larger than the critical temperature of the probe:

$$T_c(\text{probe}) < T_c(\text{powder}) \qquad (2.45)$$

As the critical temperature of niobium with T_c = 9.2K is larger than the critical temperatures of many other superconductors, one uses quite often niobium powder.

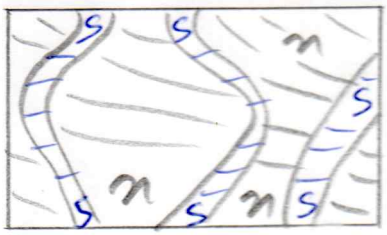

The small grains of the niobium powder represent ideal diamagnets in the superconducting state. Therefore, they are expelled from the regions of larger magnetic fields, i.e. the normal conducting regions. Thus, they gather preferably at the surface of superconducting regions. A view from the top on a planar probe then reveals meandering superconducting regions.

2.5.3 Faraday Effect:

The Faraday effect is a magneto-optical phenomenon, i.e. originates from an interaction between light and a magnetic field in a medium. More precisely, the Faraday effect causes a rotation of the plane of the polarization, which is linearly proportional to the component of the magnetic field in the direction of the propagation.

In order to observe the Faraday effect experimentally, one uses crossed polarisers. Without a magnetic field, the observed light intensity behind the crossed polarisers vanishes. But with a magnetic field in the propagation direction of light, the observed light intensity no longer vanishes. But one can rotate on polariser with a certain angle α, so that the light vanishes again. And this angle α turns out to be not only proportional to the magnetic induction B in propagation direction but also to the material width d:

$$\alpha = V d B \tag{2.46}$$

Here V denotes the Verdet constant, which is determined by the dispersion $dn/d\lambda$ of the underlying material:

$$V = \frac{e}{m} \frac{\lambda}{2c} \frac{dn}{d\lambda} \tag{2.47}$$

Here n denotes the refractive index and λ the wave length of light. Thus, we conclude that the Faraday effect is largest in the vicinity of an absorption line as then the dispersion $dn/d\lambda$ is largest. This observation allows an atomistic interpretation of the Faraday effect. In the vicinity of an absorption line the electrons oscillate resonantly with the light frequency in the polarisation direction. Thus, in presence of an additional magnetic field in propagation direction, a Lorentz force acts on the electrons, which causes them to precess with the Larmor frequency

$$\omega_L = \frac{eB}{2m} \tag{2.48}$$

And this precession causes the polarisation plane to rotate with an angle α, which can also be rewritten according to (2.46) – (2.48) via

$$\alpha = -\omega_L d \frac{\lambda}{c} \frac{dn}{d\lambda} \tag{2.49}$$

The experimental set up looks now as follows. ① represents a superconductor where surface

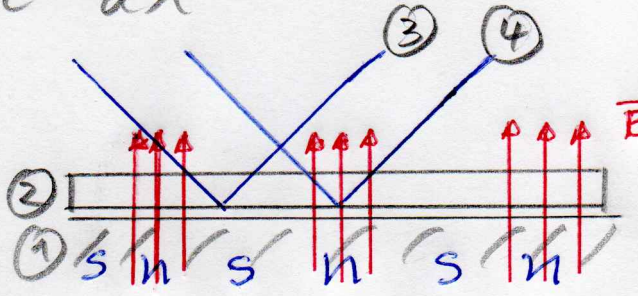

is formed to be a mirror. On top of ① we have a magneto-optically active material ②. If the light beam reflected at a superconducting mirror region ③, there is no magnetic induction due to the Meissner-Ochsenfeld effect and the polarisation plane is not changed. But if the light beam is reflected at a normal conducting region of the mirror ④, the magnetic induction there yields a rotation of the polarisation direction. In conclusion, the Faraday effect allows to distinguish between superconducting and normal conducting regions at the surface of the superconductor. One advantage of the Faraday effect in comparison with the powder method is that it also allows to detect, in principle, temporal changes of the intermediate state of type I superconductors.